Metabolically Derived Potential on the Outer Membrane of Mitochondria: A Computational Model

Sergy V. Lemeshko* and Victor V. Lemeshko†

*Department of Molecular Physiology and Biophysics, Baylor College of Medicine, Houston, Texas 77030 USA, and †Department of Physics, National University of Colombia, Medellin Branch, AA3840 Medellin, Colombia

ABSTRACT The outer mitochondrial membrane (OMM) is permeable to various small substances because of the presence of a voltage-dependent anion channel (VDAC). The voltage dependence of VDAC's permeability is puzzling, because the existence of membrane potential on the OMM has never been shown. We propose that steady-state metabolically derived potential (MDP) may be generated on the OMM as the result of the difference in its permeability restriction for various charged metabolites. To demonstrate the possibility of MDP generation, two models were considered: a liposomal model and a simplified cell model with a creatine kinase energy channeling system. Quantitative computational analysis of the simplified cell model shows that a MDP of up to −5 mV, in addition to the Donnan potential, may be generated at high workloads, even if the OMM is highly permeable to small inorganic ions, including potassium. Calculations show that MDP and ΔpH, generated on the OMM, depend on the cytoplasmic pH and energy demand rate. Computational modeling suggests that MDP may be important for cell energy metabolism regulation in multiple ways, including VDAC's permeability modulation and the effect of electrodynamic compartmentation. The osmotic pressure difference between the mitochondrial intermembrane space and the cytoplasm, as related to the electrodynamic compartmentation effects, might explain the morphological changes in mitochondria under intense workloads.

INTRODUCTION

Mitochondria play a key role in the energy metabolism of aerobic cells and are formed by two membranes. The inner mitochondrial membrane (IMM) is known to be responsible for energy transformation, and its permeability is highly selective for metabolites and ions. Accumulated data suggest that the outer mitochondrial membrane (OMM) may be important in the regulation of metabolite fluxes and energy flow between the mitochondria and the cytoplasm (Liu and Colombini, 1992a; Sorgato and Moran, 1993; Saks et al., 1993, 1995; Brdiczka and Wallimann, 1994; Rostovtseva and Colombini, 1997), but the regulatory mechanisms remain to be elucidated.

In vitro, the rate of mitochondrial oxidative phosphorylation is significantly accelerated by external endergonic reactions utilizing ATP. Respiratory acceleration by ADP in the presence of inorganic phosphate (P_i) is known as the respiratory control phenomenon. In vivo, regulation of cellular energy metabolism is more complicated. Creatine kinase (CK), adenylate kinase, hexokinase, pyruvate kinase, and nucleoside diphosphokinase enzyme systems participate in energy channeling by specific metabolite compartmentation due to the highly organized structure of the cell and mitochondria (Wallimann et al., 1992; Saks et al., 1994; Brdiczka and Wallimann, 1994; Lipskaya et al., 1995). Various aspects of energy channeling are related to the voltage-dependent anion channel (VDAC), which was discovered more than 20 years ago (Schein et al., 1976; Colombini, 1979).

The VDAC forms large (up to 3 nm in diameter) aqueous pores in the OMM (Mannella et al., 1992; Colombini et al., 1996). The pore is composed of a 30-kDa peptide, called mitochondrial porin (Colombini et al., 1996), and sometimes may constitute more than 60% of the OMM total protein (Mannella, 1982). These pores have been shown to mediate the flux of charged metabolites, which are mostly organic anions, in a voltage-dependent manner (Colombini et al., 1996; Rostovtseva and Colombini, 1997; Rostovtseva and Bezrukov, 1998). VDAC is more permeable to anions in the open state, which normally occurs at membrane potentials with absolute values lower than 10–20 mV. At potentials with absolute values higher than 20 mV, VDAC undergoes transitions to multiple closed states and becomes more selectively permeable for cations (Schein et al., 1976; Colombini et al., 1996). Synthetic polyanions (Mangan and Colombini, 1987; Colombini et al., 1987; Zizi et al., 1995), reduced pyridine nucleotides (Lee et al., 1996), a protein localized in the mitochondrial intermembrane space (MIMS) (Liu and Colombini, 1992b; Holden and Colombini, 1993), and oncotic pressure (Zimmerberg and Parsegian, 1986) modulate the voltage dependence of the porin permeability. Synthetic polyanions greatly increase the slope of VDAC's permeability-voltage (PV) characteristic (Mangan and Colombini, 1987; Colombini et al., 1987). For instance, in the presence of dextran sulfate, a 10-fold decrease in VDAC's open probability has been observed with voltage changes from 0 mV to +5 mV or from 0 mV to −5 mV (Zizi et al., 1995). Modulation by various regulatory

Received for publication 11 September 2000 and in final form 14 September 2000.

Address reprint requests to Dr. Sergy V. Lemeshko, Department of Molecular Physiology and Biophysics, Baylor College of Medicine, One Baylor Plaza, Houston, TX 77030. Tel.: 713-798-5729; Fax: 713-798-3125; E-mail: lemeshko@bcm.tmc.edu.

0006-3495/00/12/2785/16 $2.00

factors restricts VDAC's permeability to small organic anions, which may promote metabolite compartmentation. As a consequence, the rate of various mitochondrial enzymatic reactions may change.

The main question, which remains to be elucidated, is whether any mechanisms exist for electrical potential generation on the OMM, and if so, what values of the potential may be expected under physiological conditions. One possible mechanism of OMM potential (OMMP) generation may be Donnan potential (DP) (Liu and Colombini, 1992a, 1992b). Another proposed mechanism is capacitance coupling between the inner and outer membranes (Benz et al., 1990), but it has not been pursued in the literature. Some authors question the existence of a sufficiently high OMMP because many small ions, particularly potassium, are highly permeable through the OMM, and therefore they may counter any generated potential, with the exception of DP. Thus, several possible mechanisms exist which may generate the OMMP, but it has been difficult to obtain experimental evidence for any one of them.

We propose that steady-state fluxes of charged metabolites through the OMM may be the source of the OMMP. Taking into account the complexity of the cellular energy distribution system, we propose a simplified model of energy transfer in the cell for computational study. Such an approach seems to be useful for the estimation of a possible range of MDP values that may be generated on the OMM under physiological steady-state energy demand rates in rodent heart.

Computational analysis of the model showed that generated MDP can be high enough to regulate metabolite fluxes, even in the presence of physiological concentrations of highly permeable free K^+ and other small ions in the system. The model predicts electrodynamic compartmentation of charged metabolites, potassium, and other ions. The obtained results suggest that MDP on the OMM may be directly involved in the regulation of mitochondrial and cellular energy metabolism.

THE MODELS FOR METABOLICALLY DERIVED MEMBRANE POTENTIAL GENERATION

Characteristics of the steady-state model for metabolically derived potential generation on a liposomal membrane

The main principle of MDP generation may be demonstrated with the model in Fig. 1. We assume that one liposome of volume V_2 is put in a medium of infinitely large volume V_1. The liposome contains an allosteric enzyme E catalyzing an essentially irreversible reaction converting organic anion A^- to another organic anion B^-. Both anions are able to permeate the liposomal membrane. Anions A^- and B^- are added to the system in the form of potassium salts, and their initial concentrations are equal in both the internal and external mediums. Additionally, initial concentrations of KCl are also equal inside and outside of the liposome. The liposomal membrane may be considered permeable or impermeable for K^+ and Cl^-.

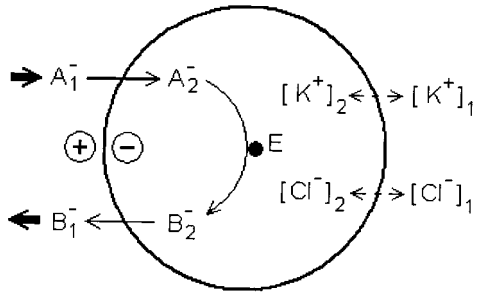

FIGURE 1 The liposomal model of steady-state MDP generation, described by Eqs. 1–15. The liposome contains KCl and enzyme E, catalyzing an essentially irreversible reaction of conversion organic anion A^- to B^-. The permeability of the liposomal membrane for A^- is higher than that for B^-. The membrane may be considered permeable or impermeable for K^+ and Cl^-. The external medium, of infinitely large volume, contains A^- and B^- in equal concentrations, which corresponds to a nonequilibrium state of the reaction (assuming that at equilibrium state $[A^-] \ll [B^-]$). Diffusional steady-state potential will be generated on the liposomal membrane, and its value will be determined by the rate of the enzymatic reaction inside the liposome, the relationship of membrane permeabilities for A^- and B^-, and the membrane permeability for K^+ and Cl^-.

Now, an activator of the allosteric liposomal enzyme E is added to increase $v_{m,l}$, the maximum rate of enzymatic conversion of A^- to B^- in the liposome (Eq. 1), which was initially equal to 0. As a result, the initially equilibrated internal concentrations $[A^-]_2 = [A^-]_1$ and $[B^-]_2 = [B^-]_1$ change because of the internal enzymatic activity. In turn, the activated conversion of A^- to B^- in the liposome will cause the influx of A^- into the liposome and the efflux of B^- from the liposome into the external medium. Membrane electrical potential will be generated because of the difference in the permeability coefficients P_A and P_B. Potassium and chloride ion concentrations inside and outside the liposome will not change if the membrane is impermeable for these ions, but their distributions will reach equilibrium if the membrane is permeable for them. It is evident that membrane permeability for K^+ and Cl^- will cause a significant decrease in the metabolically generated membrane potential. Nernstian redistribution of K^+ and Cl^-, in the case of the permeable membrane, may affect steady-state A^- and B^- fluxes, the osmotic pressure difference, and electrodynamic compartmentation of the organic ions as demonstrated by computational study of this model.

Mathematical description of the steady-state model for metabolically derived potential generation on a liposomal membrane

The model in Fig. 1 may be described mathematically in the following way. Assuming that enzymatic conversion of A^-

to B^- in the liposome is essentially irreversible and is characterized by a simple first-order Michaelis-Menten kinetics, the rate of this reaction may be described as

$$v_1 = \frac{[A^-]_2 \cdot v_{m,1}}{K_{m,2} + [A^-]_2}, \quad (1)$$

where $v_{m,1}$ is the maximum rate and $K_{m,2}$ is the Michaelis-Menten constant.

The fluxes for A^- and B^- ions across the membrane due to the difference in their concentrations $[A^-]_2$, $[A^-]_1$, and $[B^-]_2$, $[B^-]_1$, caused by enzymatic activity inside the liposome, may be expressed by Goldman's equation for ionic flux at the approximation of constant electrical field across the membrane:

$$J_A = P_A \cdot \frac{\Delta\varphi \cdot F}{RT} \cdot \frac{[A^-]_2 - [A^-]_1 \cdot e^{\Delta\varphi \cdot F/RT}}{1 - e^{\Delta\varphi \cdot F/RT}}, \quad (2)$$

$$J_B = P_B \cdot \frac{\Delta\varphi \cdot F}{RT} \cdot \frac{[B^-]_2 - [B^-]_1 \cdot e^{\Delta\varphi \cdot F/RT}}{1 - e^{\Delta\varphi \cdot F/RT}}, \quad (3)$$

where P_A is the membrane permeability coefficient for A^-, P_B is the permeability coefficient for B^-, F is the Faraday constant, $\Delta\varphi$ is the membrane potential, R is the gas constant, and $T = 310$ K is normal body temperature.

P_B was set at $0.2P_A$ to model a fivefold difference in the liposomal membrane permeabilities for A^- and B^- ions. The P_A value was varied in some range. The liposomal volume V_2 was held constant and equal to 1 μl. To consider the external volume V_1 infinitely large relative to V_2, V_1 was set at 1 ml, and the relationship between concentrations $[A^-]_1$ and $[B^-]_1$ was defined as constant and independent of the rate of A^- to B^- conversion in the liposome. The initial concentrations of A^- and B^- in the two media were set at 10 mM each. The average concentration of A^- together with B^- (the sum of the molecules A^- and B^- in the system is constant because of the 1:1 stoichiometry of the reaction in the liposome), as well as the average concentrations of added K^+ (100 mM) and Cl^- (80 mM), may be expressed by the following equations, respectively:

$$0.02\text{M} = \frac{([A^-]_1 + [B^-]_1) \cdot V_1 + ([A^-]_2 + [B^-]_2) \cdot V_2}{V_1 + V_2}, \quad (4)$$

$$0.1\text{M} = \frac{[K^+]_1 \cdot V_1 + [K^+]_2 \cdot V_2}{V_1 + V_2}, \quad (5)$$

$$0.08\text{M} = \frac{[Cl^-]_1 \cdot V_1 + [Cl^-]_2 \cdot V_2}{V_1 + V_2}, \quad (6)$$

In addition, the space-charge neutrality principle should be maintained; that is,

$$[K^+]_1 - [A^-]_1 - [B^-]_1 - [Cl^-]_1 = 0, \quad (7)$$

$$[K^+]_2 - [A^-]_2 - [B^-]_2 - [Cl^-]_2 = 0. \quad (8)$$

At steady state, the rate of A^- to B^- conversion and the fluxes of A^- and B^- across the membrane must be equal:

$$J_A = -J_B, \quad (9)$$

$$J_A = v_1. \quad (10)$$

In the case where the membrane is impermeable to K^+ and Cl^-, the following equations should be satisfied:

$$[K^+]_1 = [K^+]_2, \quad (11)$$

$$[Cl^-]_1 = [Cl^-]_2. \quad (12)$$

When the membrane is permeable for these ions, Nernstian distribution has to be observed (when the membrane potential is generated by the steady-state fluxes of A^- and B^-):

$$\Delta\varphi = -\frac{RT}{F} \cdot \ln\frac{[K^+]_2}{[K^+]_1}, \quad (13)$$

$$\Delta\varphi = \frac{RT}{F} \cdot \ln\frac{[Cl^-]_2}{[Cl^-]_1}. \quad (14)$$

The osmotic pressure difference between the liposomal matrix and the external medium may be expressed by the following equation:

$$\Delta X = [A^-]_2 + [B^-]_2 + [Cl^-]_2 + [K^+]_2 - [A^-]_1 - [B^-]_1 - [Cl^-]_1 - [K^+]_1. \quad (15)$$

The system of Eqs. 1–12 and 15, or 1–10 and 13–15, may be solved computationally, using standard software that uses numerical methods.

General characteristics of the simplified cell model

Energy transfer through the OMM of muscle cells may be represented in general as shown in Fig. 2 *A*. It includes oxidative phosphorylation, creatine kinase, adenylate kinase, and cytoplasmic ATPase systems. CK in the MIMS utilizes creatine (Cr) and ATP to produce phosphocreatine (PCr) and ADP. PCr molecules diffuse into the cytoplasm, where cytoplasmic CK utilizes them and ADP to produce ATP and Cr. Cr diffuses back into the MIMS, while ATP is used in endergonic processes by myofibrils, producing P_i, ADP, and work. In parallel, ATP may diffuse directly from the MIMS into the cytoplasm to be utilized by myofibrils. ADP, formed by hydrolysis of ATP in the cytoplasm, can be utilized by cytoplasmic CK or by adenylate kinase (AK), or diffuse into the MIMS. AMP, formed by the cytoplasmic AK reaction, diffuses into the MIMS, where the MIMS AK uses AMP and ATP to produce ADP for oxidative phosphorylation.

The general model of metabolite fluxes shown in Fig. 2 *A* could be described mathematically if the literature contained all experimental data for the components in this

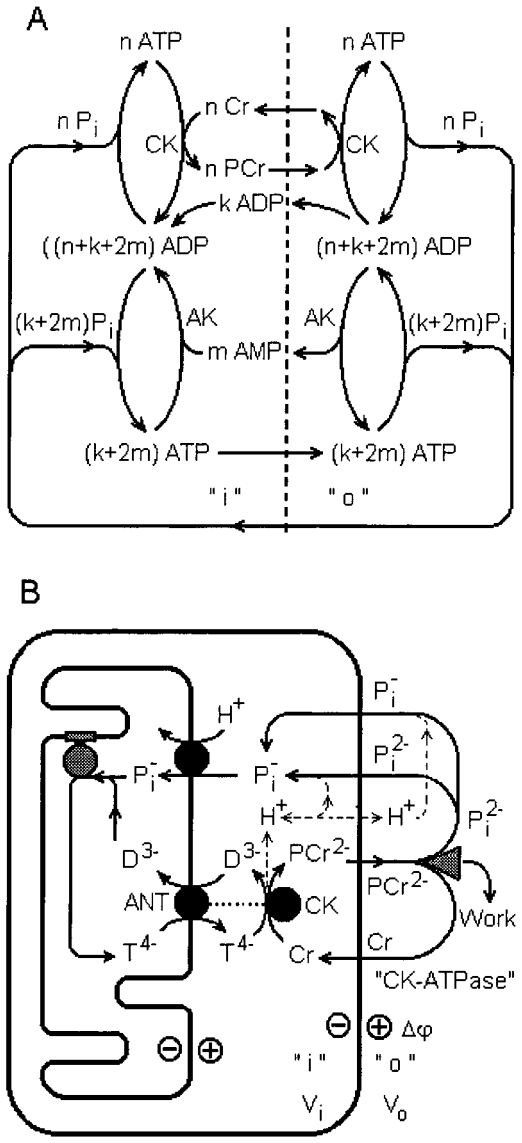

FIGURE 2 Cell model of metabolite flux between mitochondria and the cytoplasm. (*A*) Complete scheme reflecting ATP, ADP, AMP, PCr, Cr, and P_i diffusion through the OMM. (*B*) Simplified scheme, assuming that only PCr^{2-}, P_i^{2-}, P_i^-, and Cr are permeable through the OMM. D^{3-} is ADP^{3-}, T^{4-} is ATP^{4-}. The CK-ATPase system includes the cytoplasmic CK and ATPase. The OMM is permeable to small inorganic ions.

model. On the other hand, a simplified model may illustrate the basic principle of OMMP generation, by reducing the general model in Fig. 2 *A* to the model in Fig. 2 *B*, which considers only the CK system-mediated energy transfer. This system has been shown to play a key role in tissues with high and fluctuating energy demands, and many of its kinetic characteristics have been determined experimentally (Wallimann et al., 1992; Saks et al., 1993, 1994, 1995; Brdiczka and Wallimann, 1994; O'Gorman et al., 1996).

In the simplified model (Fig. 2 *B*), the charges of metabolites were included for computational estimation of the OMMP generated by the steady-state fluxes of those charged metabolites. According to this model, ATP^{4-}, formed in the matrix of mitochondria from P_i^- and ADP^{3-}, is transported into the MIMS in exchange for ADP^{3-} through the adenine nucleotide translocatior (ANT). In the MIMS, CK produces PCr^{2-} and ADP^{3-} from Cr and ATP^{4-}. ADP^{3-} is transported into the matrix through ANT to bring a new molecule of ATP^{4-} into the MIMS. PCr^{2-} diffuses into the cytoplasm and is utilized together with cytoplasmic ADP^{3-} by cytoplasmic CK to produce ATP^{4-} and Cr. Formed ATP^{4-} is utilized by myofibrils to produce P_i^-, ADP^{3-}, and work. Therefore, if we call cytoplasmic CK and ATPase a "CK-ATPase system," we may say that PCr^{2-}, diffusing into the cytoplasm from the MIMS, is "hydrolyzed" by the cytoplasmic CK-ATPase system. To close the cycle, Cr, P_i^-, and P_i^{2-} diffuse back into the MIMS, where P_i^- is transported into the mitochondrial matrix and P_i^{2-} is protonated for transport. Finally, Cr is utilized in the MIMS CK reaction for PCr^{2-} synthesis (Fig. 2 *B*).

The fluxes of ATP^{4-}, ADP^{3-}, and AMP^{2-} through the OMM are omitted in the model in Fig. 2 *B* for the purpose of simplification. This is based on the data showing that PCr^{2-} flux through the OMM is ~10 times higher than the ATP^{4-} flux in working rat heart (Saks et al., 1994). In addition, it has been shown that VDAC can significantly limit the flow of adenine nucleotides between the MIMS and the cytoplasm (Saks et al., 1993; Rostovtseva and Colombini, 1997; Hodge and Colombini, 1997). While data for PCr^{2-} permeability through VDAC are to the best of our knowledge absent from the literature, we used the experimental data of Colombini (personal communication) for open and closed states of VDAC. The data for P_i^- and P_i^{2-} permeabilities are available in the literature (Hodge and Colombini, 1997). Free potassium, chloride, and magnesium ions were included in the model at their physiological concentrations.

The creatine molecule has a net zero charge at physiological conditions. Although we did not find any experimental data about Cr permeation through VDAC or the OMM, we assumed that the OMM permeability for Cr is not a limiting factor in energy transfer between mitochondria and the cytoplasm. This assumption was based on the fact that VDAC, being a large water-filled pore, restricts its permeability for ions mostly by electrostatic mechanisms (Colombini et al., 1996). As a result, among the metabolites in Fig. 2 *A*, only the exchange of P_i^-, P_i^{2-}, and PCr^{2-} ions and the flux of noncharged Cr through the OMM were considered.

Mathematical description of the simplified cell model

The process of energy utilization, by means of the CK-ATPase system (Fig. 2 *B*) in the cytoplasm, can be de-

scribed in general by two reactions,

$$PCr_o + ADP_o \rightleftharpoons ATP_o + Cr_o, \quad (16)$$

$$ATP_o + H_2O \rightleftharpoons ADP_o + P_{i,o}, \quad (17)$$

the sum of which yields

$$PCr_o + H_2O \rightleftharpoons Cr_o + P_{i,o}. \quad (18)$$

Resultant PCr^{2-} "hydrolysis" (Eq. 18) by the cytoplasmic CK-ATPase system is a practically irreversible reaction under physiological conditions. If we assume that reaction 18 follows simple first-order Michaelis-Menten kinetics, the rate of PCr hydrolysis, v_o, can be described as

$$v_o = \frac{[PCr^{2-}]_o \cdot v_{max,o}}{K_{ocp} + [PCr^{2-}]_o}, \quad (19)$$

where $[PCr^{2-}]_o$ is the PCr^{2-} concentration in the cytoplasm, and $v_{max,o}$ is the maximum rate of PCr utilization by the CK-ATPase system in the cytoplasm. $v_{max,o}$ was scanned in a wide range of values for computational study of the model. $v_{max,o}$ is known to be modulated by Ca^{2+} during the muscle contraction cycle. The rate of PCr^{2-} hydrolysis at steady state depends on $v_{max,o}$ and on the steady-state concentration of PCr^{2-} in the cytoplasm, $[PCr^{2-}]_o$. In turn, $[PCr^{2-}]_o$ depends on the rate of Cr rephosphorylation in the MIMS and on PCr^{2-} flux through the OMM. Using Goldman's constant field approximation, PCr^{2-} flux through the OMM, $J_{PCr^{2-}}$, is described as

$$J_{PCr^{2-}} = P_{PCr^{2-}} \cdot y \cdot \frac{[PCr^{2-}]_i - [PCr^{2-}]_o \cdot e^y}{1 - e^y}, \quad (20)$$

where

$$y = \frac{2 \cdot F \cdot \Delta\varphi}{R \cdot T}. \quad (21)$$

In these equations, $P_{PCr^{2-}}$ is the OMM permeability for PCr^{2-}; $[PCr^{2-}]_i$ and $[PCr^{2-}]_o$ are PCr^{2-} concentrations in the MIMS and the cytoplasm, respectively; F is the Faraday constant; $\Delta\varphi$ is the OMMP; R is the gas constant; and $T = 310$ K is normal body temperature.

PCr production in the MIMS is described by the following reaction:

$$ATP_i + Cr_i \rightleftharpoons PCr_i + ADP_i. \quad (22)$$

ATP is produced in the matrix of mitochondria from ADP and P_i and transported into the MIMS in exchange for ADP through ANT in the IMM. For simplicity, the processes of P_i and ADP transport from the MIMS into the matrix, ATP production in the matrix from P_i and ADP, and ATP transport from the matrix into the MIMS may be described as a single reaction in the MIMS:

$$ADP_i + P_{i,i} \rightleftharpoons ATP_i + H_2O, \quad (23)$$

because there are known approximate relationships between concentrations of ATP, ADP, and P_i in the matrix and the MIMS (see Appendix A). Combining reactions 22 and 23 written for the MIMS compartment yields

$$Cr_i + P_{i,i} \rightleftharpoons PCr_i + H_2O. \quad (24)$$

This cumulative reaction is driven by mitochondrial oxidative phosphorylation and is essentially reversible, requiring the use of the next equation (derived in Appendix A) for the rate of PCr_i production in the MIMS, v_i:

$$v_i = \frac{\frac{v_{max,m} \cdot (41667 \cdot [P_i]_i - 19.5) \cdot 0.01 \cdot [Cr]_i}{(41667 \cdot [P_i]_i + 30.5) \cdot 7.8 \cdot 10^{-7}} - 137 \cdot [PCr^{2-}]_i \cdot v_{max,i,r}}{67.7 + 12{,}890 \cdot [Cr]_i + 1541 \cdot [PCr^{2-}]_i}, \quad (25)$$

where $v_{max,m} = 0.0067$ fmol/s, the maximum rate of ATP production by an average rat heart mitochondrion in the coupled "oxidative phosphorylation-ANT-MIMS creatine kinase" system. $[P_i]_i$ is the sum of P_i^- and P_i^{2-} concentrations in the MIMS, and $v_{max,i,r} = 0.0133$ fmol/s is the maximum rate of the reverse CK reaction in an average rat heart mitochondrion (see Appendix A), i.e., the reaction of Cr and P_i production in the MIMS from PCr. $v_{max,i,r}$ is evidently overestimated because it only corresponds to the reversed CK reaction. It may be smaller for the cumulative reaction (Eq. 24), which will lead to a higher MDP.

The flux of P_i^{2-} through the OMM may be described by an equation similar to Eq. 20, using Goldman's approximation. The P_i^{2-} flux is dependent on the OMM permeability for P_i^{2-} ($P_{P_i^{2-}}$), on P_i^{2-} concentrations in the MIMS ($[P_i^{2-}]_i$) and the cytoplasm ($[P_i^{2-}]_o$), and on the steady-state OMMP according to the following equation:

$$J_{Pi^{2-}} = P_{Pi^{2-}} \cdot y \cdot \frac{[Pi^{2-}]_i - [Pi^{2-}]_o \cdot e^y}{1 - e^y}, \quad (26)$$

where y is defined in Eq. 21.

The flux of P_i^- through the OMM may be described in the same manner:

$$J_{Pi^-} = P_{Pi^-} \cdot \frac{y}{2} \cdot \frac{[Pi^-]_i - [Pi^-]_o \cdot e^{y/2}}{1 - e^{y/2}}. \quad (27)$$

At steady state, the rates of PCr^{2-} production, PCr^{2-} efflux from the MIMS into the cytoplasm, PCr^{2-} utilization by the CK-ATPase system in the cytoplasm, and the flux of P_i through the OMM from the cytoplasm into the MIMS should all be equal. The steady-state boundary conditions can be set in the following three equations:

$$J_{Pi} = -J_{PCr}, \quad (28)$$

$$v_i = J_{Pi}, \quad (29)$$

$$v_o = J_{PCr}, \quad (30)$$

where

$$J_{Pi} = J_{Pi^{2-}} + J_{Pi^{-}}. \quad (31)$$

The minus sign in Eq. 28 appears because P_i and PCr^{2-} flow in opposite directions.

From Eqs. 28–30, the steady-state metabolite flux through the OMM of a single mitochondrion, J, can be defined as

$$J = J_{Pi} = v_i = -J_{PCr} = -v_o. \quad (32)$$

In addition to PCr^{2-}, P_i^{2-}, and P_i^{-} (see Appendix A for pK_{a2} and pH), physiological concentrations of free K^+, Cl^-, and Mg^{2+} ions were included. To have a sufficient concentration of counterions for physiological concentrations of K^+ and Mg^{2+}, arbitrary anions W^- were included in the system (see details below), as well as impermeable macromolecules Z^{20-} with the arbitrary charge 20−. Z^{20-} anions represent some equivalent of the negatively charged surface of membranes and impermeable negatively charged macromolecules. The Donnan potential was modeled by setting different concentrations of nonpermeating macromolecules Z^{20-} in the MIMS and the cytoplasm.

The Nernst equation is applied to describe the distribution of freely permeating ions K^+, Cl^-, Mg^{2+}, and H^+ between the cytoplasm and the MIMS:

$$\Delta\varphi = \frac{R \cdot T}{F} \cdot \ln \frac{[K^+]_o}{[K^+]_i}, \quad (33)$$

$$\Delta\varphi = \frac{R \cdot T}{F} \cdot \ln \frac{[Cl^-]_i}{[Cl^-]_o}, \quad (34)$$

$$\Delta\varphi = \frac{R \cdot T}{2 \cdot F} \cdot \ln \frac{[Mg^+]_o}{[Mg^+]_i}, \quad (35)$$

$$\Delta\varphi = \frac{R \cdot T}{F} \cdot \ln \frac{[H^+]_o}{[H^+]_i}. \quad (36)$$

The model is closed; i.e., it does not lose or gain any ions from the outside. Thus average ion concentrations were defined in the system using the following equations:

$$[K^+] = \frac{[K^+]_i \cdot V_i + [K^+]_o \cdot V_o}{V_i + V_o}, \quad (37)$$

$$[Cl^-] = \frac{[Cl^-]_i \cdot V_i + [Cl^-]_o \cdot V_o}{V_i + V_o}, \quad (38)$$

$$[Mg^{2+}] = \frac{[Mg^{2+}]_i \cdot V_i + [Mg^{2+}]_o \cdot V_o}{V_i + V_o}, \quad (39)$$

$$[PCr^{2-}] = \frac{[PCr^{2-}]_i \cdot V_i + [PCr^{2-}]_o \cdot V_o}{V_i + V_o}, \quad (40)$$

$$[P_i] = \frac{[P_i]_i \cdot V_i + [P_i]_o \cdot V_o}{V_i + V_o}, \quad (41)$$

where V_i and V_o are the MIMS and the cytoplasm volumes, respectively, and

$$[P_i] = [P_i^{2-}] + [P_i^{1-}]. \quad (42)$$

According to the space-charge neutrality principle, the total charge of cations is equal to the total charge of anions in a given volume (if the membrane electric capacity is negligibly small):

$$[K^+]_i + 2 \cdot [Mg^{2+}]_i + [H^+]_i - [Cl^-]_i - 2 \cdot [PCr^{2-}]_i - 2 \cdot [P_i^{2-}]_i - [P_i^{1-}]_i - 3 \cdot [ADP^{3-}]_i - 4 \cdot [ATP^{4-}]_i - [W^-]_i - 20 \cdot [Z^{20-}]_i = 0 \quad (43)$$

$$[K^+]_o + 2 \cdot [Mg^{2+}]_o + [H^+]_o - [Cl^-]_o - 2 \cdot [PCr^{2-}]_o - 2 \cdot [P_i^{2-}]_o - [P_i^{1-}]_o - 3 \cdot [ADP^{3-}]_o - 4 \cdot [ATP^{4-}]_o - [W^-]_o - 20 \cdot [Z^{20-}]_o = 0. \quad (44)$$

Making $v_{max,o} = 0$ fmol/s for the equilibrium state and using the average concentrations (see also Appendix A) $[K^+] = 150$ mM, $[Mg^{2+}] = 1$ mM, $[Cl^-] = 5$ mM, $[PCr^{2-}] = 19$ mM, $[P_i^{2-}] = 0.34$ mM and $[P_i^-] = 0.21$ mM (for $pK_{a2} = 7.2$ and pH = 7.0), $[ADP^{3-}] = 0.04$ mM, and $[ATP^{4-}] = 10$ mM, $[W^-]$ was found to be 8 mM by utilizing Eqs. 43 and 44 to maintain the space-charge neutrality principle, when concentrations of $[Z^{20-}]$ in the MIMS and in the cytoplasm were 3 mM to model DP = 0 mV. To model a nonzero DP, $[Z^{20-}]_i$ was set at 5 mM and $[Z^{20-}]_o$ was set at 3 mM. In this case, $[W^-]$ was calculated to be around 5 mM (at $v_{max,o} = 0$).

To satisfy Eqs. 43 and 44, the floating concentrations of W^-, originating from the dissociation of a week acid WH, were included in the system. The dissociation constant of WH was assumed to be the same in the MIMS and the cytoplasm:

$$\frac{[H^+]_o \cdot [W^-]_o}{[WH]_o} = \frac{[W^-]_i \cdot [H^+]_i}{[WH]_i} = K_{a,W}.$$

If WH is infinitely permeable across the OMM, then $[WH]_i = [WH]_o = [WH]$, which yields the following equation, regardless of whether W^- ion is permeable or not:

$$\frac{[H^+]_o}{[H^+]_i} = \frac{[W^-]_i}{[W^-]_o}.$$

Or, taking into account Eq. 36, it yields

$$\Delta\varphi = \frac{R \cdot T}{F} \cdot \ln \frac{[W^-]_i}{[W^-]_o}. \quad (45)$$

Thus, W^- ions will be distributed across the OMM according to the Nernst equation if electrochemical equilibrium exists for protons across the OMM. The pH_o was set and the system of equations was allowed to find the concentrations of W^- to satisfy the space-charge neutrality principle of

each medium for various steady states of the model. The space-charge neutrality principle must be satisfied because of the extremely low electrical capacity of the outer membrane.

The floating concentration [W^-] depends on the steady state and on the value of the external pH (pH_o), which is taken to be constant. Higher energy demand in the cytoplasm will lead to higher steady-state concentrations of P_i^- and P_i^{2-} in the system. P_i^{2-} is supplied from PCr^{2-} "hydrolysis," and P_i^- appears to be due to the protonation of some of the P_i^{2-}, according to pK_{a2}, fixed pH_o, and settled pH_i, by utilizing H^+ ions originating from week acid WH dissociation, which increases the concentration of W^- in the system.

Values for $v_{max,o}$ were varied from 0 to 8×10^{-3} fmol/s, covering and exceeding the physiological range of workloads related to one average mitochondrion in rat heart (see Appendix A). The average MIMS volume of rat heart single mitochondrion was taken as $V_i = 0.03$ fl (see Appendix B). The sum of cytoplasmic and myofibrillar compartment volumes, $V_o = 0.36$ fl, was chosen to be in proportion to the MIMS volume of 12:1 (see Saks and Aliev, 1996). The cytoplasmic volume V_o was set as a constant ($V_o = 12V_i$), even in the case when an osmotic pressure difference appeared between the MIMS and the cytoplasm compartments.

Critical parameters for MDP generation are the OMM permeabilities for P_i^-, P_i^{2-}, and $P_{PCr^{2-}}$. Experimentally measured ion fluxes of P_i^-, P_i^{2-}, and $P_{PCr^{2-}}$ (in 10^6 ions/s) through a single VDAC reconstituted into the planar phospholipid membrane under standard conditions are 14.0, 6.30, and 3.90, respectively, in the open state and 1.60, 0.29, and 0.24, respectively, in the closed state. The VDAC ion flux values for P_i^- and P_i^{2-} were taken from the literature (Hodge and Colombini, 1997); and the data for PCr^{2-} were kindly provided by Dr. Colombini (personal communication). These data were used to obtain the relationship of the OMM permeabilities for the metabolites above, taking all of them relative to the OMM permeability for P_i^- in the VDAC open state (Table 1).

To model the form of the experimentally determined permeability-voltage (PV) characteristics of the VDAC (Zizi et al., 1998), the following mathematical approximation was used:

$$P = a_0 \cdot [P_c + (P_o - P_c) \cdot e^{-[a(\Delta\varphi+\delta)]^2}], \qquad (46)$$

where P is the OMM absolute permeability of a single average mitochondrion for an ion, and P_o and P_c are the OMM relative permeabilities corresponding to the VDAC's open and closed states, respectively (Table 1). The absolute permeability coefficient a_0 in Eq. 46 was set at 3.6 fl/s for all calculations (Appendix B). The voltage-sensitive part of the absolute permeability function will lie between a_0P_c and a_0P_o. Higher values of a_0 would lead to a dramatic decrease in MDP, while lower values of a_0 would lead to a nonphysiological restriction of metabolite flux through the OMM (see Appendix B for more details) and to a higher value of MDP. The value of coefficient a in Eq. 46 allows an adequate bell-shaped and symmetrical PV characteristic of the VDAC. The higher the a, the steeper the slope of VDAC's permeability dependence on the OMMP. Constant δ shifts the PV curve to the left or to the right under the influence of various factors, but it was set at 0 in all calculations. In Eq. 46, δ and $\Delta\varphi$ are expressed in volts, where $\Delta\varphi$ is the OMMP (i.e., MDP in the case where DP = 0 or a combination of MDP and DP). Fig. 3 shows three symmetrical PV characteristics of the VDAC, modeled by Eq. 46, where $a_0 = 3.6$ fl/s, $a = 300\ V^{-1}$, $\delta = 0$. Fig. 3 demonstrates how DP may change permeabilities and how they can be modulated by MDP.

The difference in osmotic pressure between the MIMS and the cytoplasm needs to be considered as an additional parameter ΔX, which is calculated using the following

TABLE 1 The OMM relative permeabilities for P_i^-, P_i^{2-}, and PCr^{2-} in the open (P_o) and closed (P_c) states of the VDAC, corresponding to the relationship between experimentally determined fluxes of P_i^-, P_i^{2-} (Hodge and Colombini, 1997), and PCr^{2-} (Colombini's unpublished data) through a single VDAC reconstituted in planar phospholipid membranes

The OMM relative permeabilities in the open (P_o) and closed (P_c) states of the VDAC	Metabolites		
	P_i^-	P_i^{2-}	PCr^{2-}
P_o	1.00	0.45	0.27
P_c	0.11	0.02	0.017

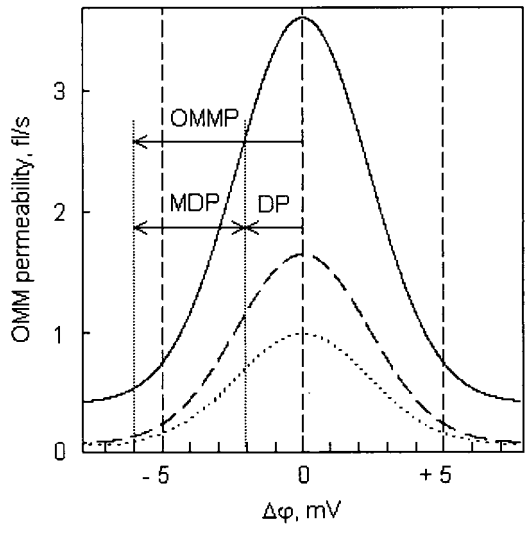

FIGURE 3 Permeability-voltage characteristics of VDAC (in fl/s) modeled by Eq. 46 for P_i^- (——), P_i^{2-} (– – –), and PCr^{2-} (· · · ·). In all plots $a_0 = 3.6$ fl/s, $a = 300\ V^{-1}$, and $\delta = 0$. Relative permeability coefficients of the OMM for P_i^-, P_i^{2-}, and PCr^{2-} in open (P_o) and closed (P_c) states of the VDAC are presented in Table 1. Permeabilities may be changed by the DP and further modulated by MDP. The DP and MDP form the OMMP.

equation:

$$\Delta X = [K^+]_i + [PCr^{2-}]_i + [Cr]_i + [P_i^{2-}]_i + [P_i^-]_i + [ADP^{3-}]_i + [ATP^{4-}]_i + [Cl^-]_i + [Mg^{2+}]_i + [W^-]_i + [Z^{20-}]_i - [K^+]_o - [PCr^{2-}]_o - [Cr]_o - [P_i^{2-}]_o - [P_i^-]_o - [ADP^{3-}]_o - [ATP^{4-}]_o - [Cl^-]_o - [Mg^{2+}]_o - [W^-]_o - [Z^{20-}]_o. \quad (47)$$

Parameter ΔX is important for morphological changes in mitochondria accompanying their metabolic state variations. The system of equations with the parameters described above was solved numerically using Mathcad 8.0 software (MathSoft, Cambridge, MA).

RESULTS

Computational analysis of the liposomal model (Fig. 1) showed that enzymatic conversion of metabolite A^- to metabolite B^- inside the liposome led to the generation of membrane potential (Fig. 4 *A*), under the following conditions: 1) when permeability coefficients of the membrane were different for these two metabolites and 2) concentrations $[A^-]_1$ and $[B^-]_1$ (in the external medium) were maintained to be essentially constant at steady state ($[A^-]_1 = [B^-]_1$). The value of MDP depended on the rate of the enzymatic reaction modulated by changing $v_{m,l}$ in Eq. 1. In a real system, an allosteric enzyme may be modulated by its allosteric activator, for example, by Ca^{2+}. MDP was significantly diminished because of Nernstian redistribution of the other permeable ions (K^+ and Cl^- in the considered liposomal model). An increase in metabolite flux J (Fig. 4 *B*) and the effect of electrodynamic compartmentation of metabolites (Fig. 4 *C*) are observed as well, when the membrane is considered permeable for K^+ and Cl^-. MDP led to an osmotic pressure difference between the liposomal matrix and the external medium through K^+ and Cl^- Nernstian redistribution and because of electrodynamic compartmentation of the metabolites (Fig. 4 *D*). Not only the ratio of

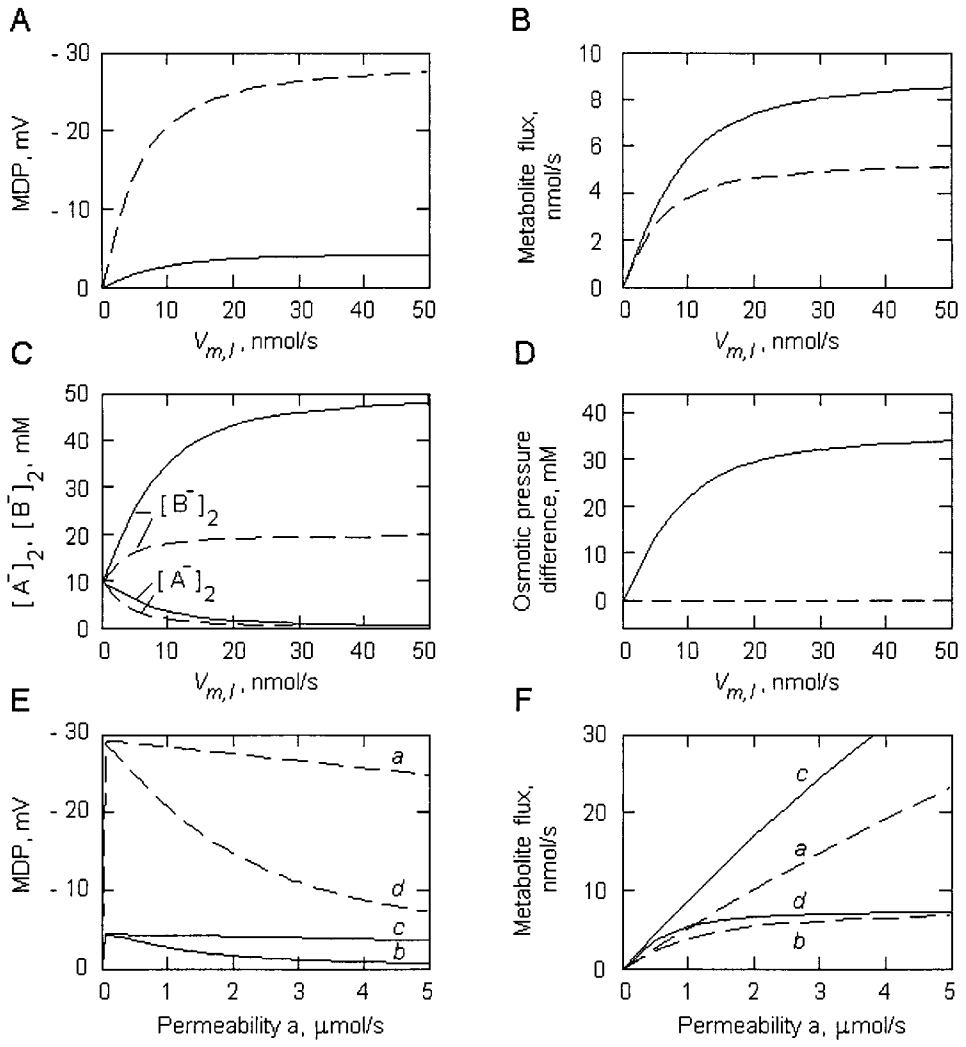

FIGURE 4 Solutions of the liposomal model for steady-state MDP generation (Fig. 1) described by Eqs. 1–15. (*A*) MDP dependence on the maximum rate of A^- to B^- conversion in the liposome, $v_{m,l}$. (*B*) Flux J of A^- or B^- dependence on $v_{m,l}$ (the fluxes of A^- and B^- are equal at steady state). (*C*) Dependence of A^- and B^- concentrations in the liposome on $v_{m,l}$. (*D*) Dependence of osmotic pressure difference between the liposome and external medium on $v_{m,l}$. (*E*) MDP dependence on the permeability coefficient a, where $P_A = a$ and $P_B = 0.2a$. (*F*) Flux J of A^- or B^- dependence on permeability coefficient P_A, where $P_B = 0.2P_A$. For *A–D*: $P_A = 1.0$ μl/s and $P_B = 0.2$ μl/s. For *E* and *F*: $v_{m,l} = 100$ nmol/s (*a*, *c*) and $v_{m,l} = 10$ nmol/s (*b*, *d*). The liposomal membrane is permeable (——, Eqs. 13 and 14 are used) or impermeable (– – –, Eqs. 11 and 12 are used) for K^+ and Cl^- ions.

membrane permeabilities for A^- and B^-, but their absolute permeabilities as well, were essential for MDP (Fig. 4 *E*) and metabolite flux (Fig. 4 *F*) dependence on the rate of liposomal enzymatic reaction.

In computational analysis of the simplified cell model (Fig. 2 *B*), the OMM permeability was assumed to be the main limiting step in metabolite flux, as long as the rate of energy demand in the cytoplasm or ATP production by mitochondria were not limiting. Dependence of the generated OMMP on the rate of PCr "hydrolysis" in the cytoplasm at pH_o 7.0 was calculated under conditions where the OMM was permeable for all ions, except nonpermeating macromolecules Z^{20-} (Fig. 5). Zero values were assigned to a in Eq. 46 when the voltage dependence of VDAC permeability was not considered. The "basic relationship" of the OMM permeabilities for P_i^-, P_i^{2-}, PCr^{2-} (Table 1) and a_0 = 3.6 fl/s were used in Eq. 46.

At DP = 0 mV (i.e., at $[Z^{20-}]_i$ = 3 mM, $[Z^{20-}]_o$ = 3 mM) and at the maximum rate of PCr^{2-} utilization in the cytoplasm ($v_{max,o}$ = 0.01 fmol/s), MDP = −0.8 mV was calculated for the case of no voltage dependence of the OMM permeability, i.e., at a = 0 V^{-1} in Eq. 46 (Fig. 5 *A*, *a*). Almost the same result, MDP = −0.9 mV, was obtained after inclusion of the PV characteristics of the VDAC, i.e., at a = 300 V^{-1} (Fig. 5 *A*, *b*). Under the same conditions, if the OMM was assumed to be impermeable for K^+, Mg^{2+}, and Cl^-, MDP equaled −3.2 mV (for a = 0 V^{-1}) and −19.6 mV (for a = 300 V^{-1}) at $v_{max,o}$ = 0.01 fmol/s.

As a result of infinite permeability of the OMM for K^+, Mg^{2+}, and Cl^- ions, only a small value of MDP may be generated on the OMM. However, the steady-state metabolite flux J under the maximum rate of energy demand in the cytoplasm (Fig. 5 *B*, *b*) is nearly 240% (for a = 300 V^{-1}) of that calculated for the OMM impermeable for K^+, Mg^{2+}, and Cl^- ions under the same conditions (data not shown). The latter effect is similar to that observed in the liposomal model (Fig. 4). In addition, the calculated MDP value seems to be high enough to modulate the energy flux

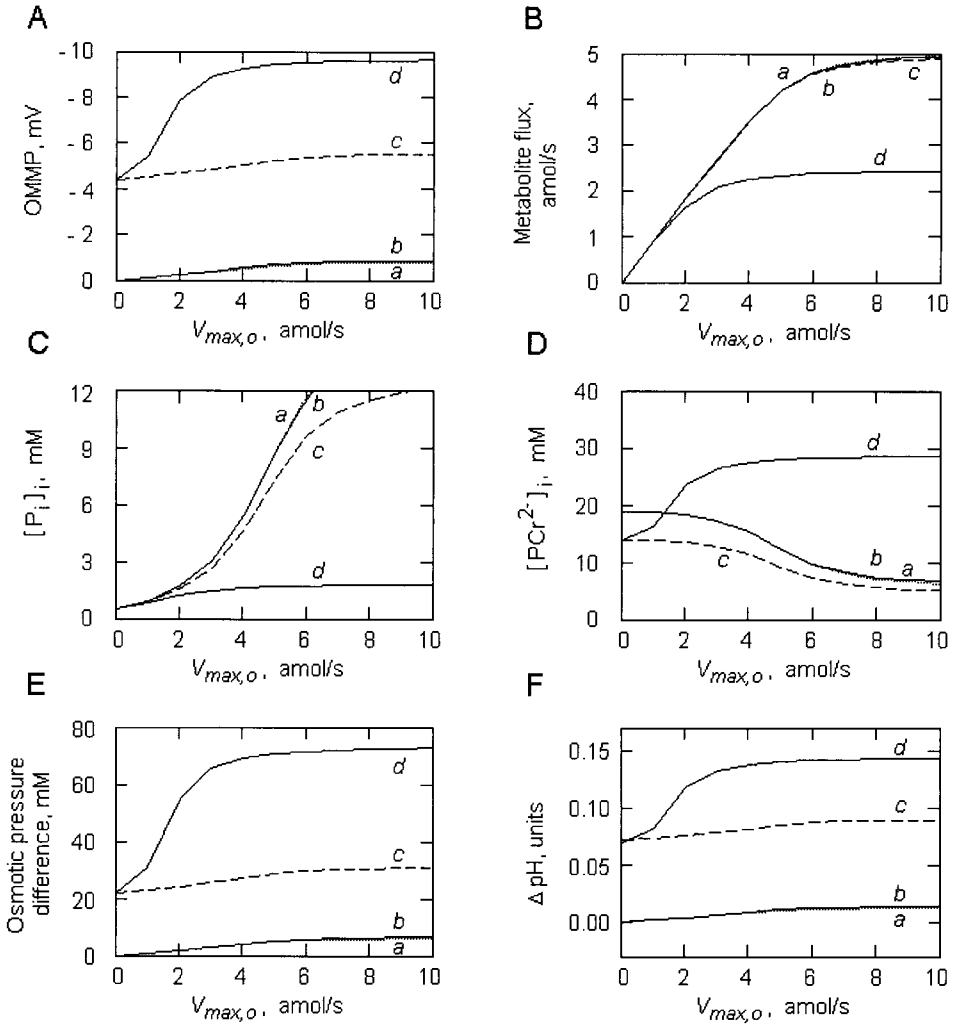

FIGURE 5 Calculated dependence of the OMMP (*A*), metabolite flux (*B*), P_i concentration in the MIMS (*C*), PCr^{2-} concentration in the MIMS (*D*), osmotic pressure difference (*E*), and ΔpH (*F*) between the MIMS and the cytoplasm on the maximum rate of PCr utilization in the cytoplasm ($v_{max,o}$) at pH_o 7.0 and DP = 0 mV (*a*, *b*) or DP = −4.4 mV (*c*, *d*). The relationship of the permeability coefficients for P_i^-, P_i^{2-}, and PCr^{2-} is taken from Table 1; a_0 = 3.6 fl/s, a = 0 V^{-1} (*a*, *c*) or a = 300 V^{-1} (*b*, *d*), δ = 0 V (see Eq. 46).

through the OMM, when these changes occur at the slope of the VDAC's permeability dependence on the membrane electric potential (Fig. 3).

So far, MDP generation was considered at DP = 0. Inclusion of DP would diminish the OMM permeability for various metabolites and shift the VDAC's PV characteristics to a region of greater dependence of the VDAC's permeability on MDP (see Fig. 3). The system of equations, describing the simplified cell model, allows modeling of the DP in addition to MDP. In this case, the total OMMP is the sum of MDP and the DP (Fig. 3). To model DP = −4.4 mV (Fig. 5 *A*, *c* and *d*), $[Z^{20-}]_i$ = 5 mM and $[Z^{20-}]_o$ = 3 mM were included in the system, as opposed to $[Z^{20-}]_i$ = 3 mM and $[Z^{20-}]_o$ = 3 mM, taken for DP = 0. In both cases, the OMM was assumed to be infinitely permeable for K^+, Mg^{2+}, W^-, Cl^-, and H^+. The value of DP = −4.4 mV corresponds to a zero rate of energy demand in the cytoplasm ($v_{max,o} = 0, J = 0$). By shifting the PV characteristics of the VDAC to their highest sensitivity to the OMMP (Fig. 3), the DP allows generation of a relatively high MDP. For example, the OMMP up to −9.5 mV (i.e., MDP = −5.1 mV and DP = −4.4 mV) is calculated under the maximum rate of PCr^{2-} "hydrolysis" in the cytoplasm at pH_o 7.0 and $a = 300\ V^{-1}$ (Fig. 5 *A*, *d*). In the absence of the OMM permeability dependence on the OMMP ($a = 0\ V^{-1}$), only a small value of MDP, in addition to the DP, is generated, yielding the OMMP = −5.5 mV (Fig. 5 *A*, *c*). In the latter case, the MDP value (−1.1 mV) is similar to that observed under the conditions where DP = 0 mV, with (Fig. 5 *A*, *b*) or without (Fig. 5 *A*, *a*) the voltage dependence of the OMM permeability.

MDP, as the part of the OMMP, leads to a dramatic change in energy flux *J* dependence on the workload under the conditions above (Fig. 5 *B*, *d*). This effect may have a physiological relevance, for it may protect mitochondria from the work overload, because elevated concentrations of Ca^{2+} and P_i in the cytoplasm, and consequently in the MIMS, may induce inner membrane permeability transition when the inner membrane potential is diminished for any reason.

Redistribution of metabolites between the MIMS and the cytoplasm at steady state is observed as a result of MDP generation on the OMM (electrodynamic compartmentation effect). For example, the MIMS concentrations of P_i (Fig. 5 *C*, *d*) and PCr^{2-} (Fig. 5 *D*, *d*) change dramatically when a high MDP is generated (at DP = −4.4 mV, $a = 300\ V^{-1}$).

As a result of the Nernstian redistribution of permeating ions and electrodynamic compartmentation of metabolites supported by the OMMP, an increase in the MIMS osmotic pressure appears under a high rate of PCr utilization in the cytoplasm (Fig. 5 *E*). Calculations above were done without consideration of possible MIMS volume changes under the influence of osmotic pressure increase in the MIMS. If such volume changes take place, they may further modulate the energy flux in the system, for example, through dilution of the metabolites in the MIMS. It may also change the OMM permeability through dilution of some VDAC modulators and/or through mechanical stress on the OMM. Furthermore, increased osmotic pressure in the MIMS may lead to decreased mitochondrial matrix volume and increased mechanical stress on the OMM.

Nernstian electrochemical equilibration of H^+ ions on the OMM due to the OMMP leads to the MIMS acidification relative to the cytoplasm (Fig. 5 *F*). The OMM ΔpH value is higher under high rates of energy demand in the cytoplasm (Fig. 5 *F*, *d*). At the same time, Nernstian redistribution of permeating ions, such as K^+ and Mg^{2+}, leads to their dramatic accumulation in the MIMS under MDP generation. For example, at OMMP = −9.5 mV (MDP plus DP) generated under $v_{max,o}$ = 0.006 fmol/s (Fig. 5 *A*), the equilibrated concentrations of K^+ and Mg^{2+} in the MIMS were calculated to be 207 mM and 1.89 mM, respectively, while under zero workload ($v_{max,o}$ = 0, DP = −4.4 mV) they were 175 mM and 1.35 mM, respectively. Thus, MDP generation was accompanied by an 18% increase in K^+ concentration and a 40% increase in Mg^{2+} (as well as Ca^{2+}) concentration in the MIMS, compared with that observed under zero workload. Computational data in Fig. 5 demonstrate that the voltage dependence of the VDAC's permeability, as well as the DP, is important for relatively high MDP generation on the OMM, for osmotic and electrodynamic compartmentation effects, and, as a whole, for energy flux regulation in the cell.

The rate of ATP production by mitochondria for the MIMS-CK reaction may be modulated by ANT activity through the OMMP-dependent change in adenine nucleotides and Mg^{2+} concentrations in the MIMS. In this model, the possible direct influence of such modulation on MDP was not considered. Instead, any such influence was simulated by varying the maximum rate of ATP production for the MIMS-CK reaction in a wide range, that is, taking $v_{max,m}$ to be equal to 0.001 fmol/s and 0.003 fmol/s in addition to $v_{max,m}$ = 0.0067 fmol/s (see Eqs. 25 and A12). Obtained data show that even when $v_{max,m}$ decreases almost 7 times, generated MDP may be sufficiently high (Table 2) for the OMM permeability regulation at a high rate of PCr^{2-} "hydrolysis" in the cytoplasm ($v_{max,o}$ = 0.005 fmol/s). For instance, when $v_{max,m}$ decreases 6.7 times, metabolite flux decreases only 3.4 times (Table 2), at pH_o 7.0.

A significant change in the cytoplasmic pH may occur under some physiological and pathological conditions. The simplified cell model allows modeling of the pH behavior of the system, specifically MDP generation dependence on pH in the cytoplasm. The calculations in Table 2 show that pH has a significant effect on MDP. On the other hand, a pH difference of nearly −0.2 units may be generated across the OMM under maximum workloads (Table 2).

In general, calculations clearly show that negative MDP may be generated on the OMM at steady state, in addition to the DP. MDP and the ΔpH difference between the cyto-

TABLE 2 Dependence of the OMMP (DP and MDP), metabolite flux (J), osmotic pressure difference (ΔX), and ΔpH between the MIMS and the cytoplasm ($\Delta pH = pH_{MIMS} - pH_{cyt}$) on the maximum rate of ATP production by mitochondria ($v_{max,m}$; see Eq. 25), and on the cytoplasmic pH (pH_o) at the fixed maximum rate of the energy demand in the cytoplasm, $v_{max,o} = 0.005$ fmol/s (see Eq. 25), and DP = −4.4 mV

Maximum rate of ATP production ($v_{max,m}$) and pH_o	DP+MDP (mV)	J (amol/s)	ΔX (mM)	ΔpH
$v_{max,m}$ = 0.0067 fmol/s				
pH_o 6,5	−7.3	1.9	49	−0.12
pH_o 7,0	−9.5	2.4	71	−0.15
pH_o 7,5	−11.0	2.8	87	−0.18
$v_{max,m}$ = 0.003 fmol/s				
pH_o 6,5	−6.8	1.6	44	−0.11
pH_o 7,0	−8.5	1.7	60	−0.14
pH_o 7,5	−9.3	1.8	68	−0.15
$v_{max,m}$ = 0.001 fmol/s				
pH_o 6,5	−5.4	0.7	30	−0.09
pH_o 7,0	−6.14	0.7	37	−0.10
pH_o 7,5	−6.6	0.7	40	−0.11

The value of DP = −4.4 mV is modeled by $[Z^{20-}]_i$ = 5 mM, and $[Z^{20-}]_o$ = 3 mM, leading to ΔX = 22 mM and ΔpH = 0.07 at $v_{max,o} = 0$, regardless of $v_{max,m}$ and pH_o values. The permeability coefficients relationship was taken as in Table 1, with a_0 = 3.6 fl/s, a = 300 V^{-1}, and $\delta = 0$ (see Eq. 46).

plasm and the MIMS increase at higher workloads. The DP may be important for regulation of the VDAC's permeability by MDP, because the DP allows a shift of the VDAC's PV characteristics to a region of greater dependence of the permeability on the OMMP, a part of which is MDP. This computational study of the simplified cell model shows that a realistic possibility exists for electrical potential generation on the OMM because of the flux of charged metabolites, despite the OMM's high permeability for K^+. MDP is predicted to play an important role in energy metabolism regulation, electrodynamic compartmentation of metabolites, and morphological changes of mitochondria in physiological conditions.

DISCUSSION

The physiological role of the OMM in cellular energy metabolism has been studied extensively in the past decade. Although the OMM is porous, it may restrict its permeability to many metabolites with uncompensated charge. Various mechanisms for the OMM permeability regulation may exist at the level of the VDAC. Modulation of the VDAC's permeability may be achieved by at least one MIMS protein (Liu and Colombini, 1992b; Holden and Colombini, 1993), by a protein factor "x" of the cytoplasm (Saks et al., 1995), through structurally organized energy channeling (Wallimann et al., 1992; Saks et al., 1994; Brdiczka and Wallimann, 1994; Lipskaya et al., 1995), and by other factors. The OMMP may also play an important role, but the possible mechanisms of its generation are not yet known, with the exception of the DP (Liu and Colombini, 1992a, 1992b).

Many metabolites participating in energy transformation and in intracellular energy transfer are anions that pass across the OMM. The difference in the OMM permeability for such metabolites may lead to steady-state or transition-state generation of MDP. The MDP value may depend on the rate of energy utilization in the cytoplasm. MDP generated on the OMM, in accordance with the proposed mechanism, may be essential for the regulation of energy metabolism in the cell. So far, this aspect has not been analyzed in detail in the literature, mainly because the OMM has a high permeability for small ions, especially for potassium, the most abundant free ion in the cytoplasm. High permeability of the OMM for small ions was naturally assumed to cause the negation of any generated OMMP, but not the DP. It has never been determined if an electrical shortening effect by potassium and other ions is large enough to cause a complete negation of any potential generated by steady-state diffusion of charged metabolites across the OMM. To illustrate the main idea of MDP, at first the simplest liposomal model (Fig. 1) was considered.

Computational analysis of the liposomal model, described by only 13 equations, shows that membrane potential, dependent on the rate of enzymatic conversion of one charged metabolite to another, may be generated in the case of different values of membrane permeability for these metabolites (Fig. 4). Although infinite membrane permeability for potassium and chloride ions leads to a dramatic decrease in the metabolically generated potential, effects of electrodynamic compartmentation of metabolites and an increase in their flux across the membrane take place under such conditions. As a result, a significant osmotic pressure difference between the liposome and the medium is observed because of MDP generation (Fig. 4). These results suggest that similar mechanisms may exist in real cells and may be essential for the regulation of energy metabolism.

The possibility of MDP generation was also estimated in a more realistic system, by considering the simplified model of the cell with CK mediated energy channeling. The proposed model (Fig. 2 *B*) includes many kinetic parameters for mitochondrial CK that were obtained experimentally by other authors (see Aliev and Saks, 1994, and references therein), as well as some general characteristics of rat heart energy metabolism (see Appendix A). Computational study of the model shows that relatively high steady-state MDP and ΔpH may be generated on the OMM in a pH-dependent manner by the high rate of energy utilization in the cytoplasm. The MDP value depends on the absolute and relative permeabilities of the OMM for P_i^-, P_i^{2-}, and PCr^{2-}, which should be modulated by MDP according to the known PV characteristics of the VDAC shown in one particular form in Fig. 3. Unlimited OMM permeability for K^+, Mg^{2+}, and Cl^- leads to a significant drop in MDP. But even in this case, the calculations demonstrate that steady-state MDP

may be sufficiently high to be important for the regulation of metabolite flux across the OMM under high workloads. Thus, under realistic conditions of OMM permeability, MDP may reach a value around −5 mV. VDAC modulators localized in the MIMS are capable of significantly increasing the VDAC's voltage sensitivity (Liu and Colombini, 1992b; Holden and Colombini, 1993). Under some conditions, even a 0.5-mV voltage change remarkably influences VDAC permeability (Colombini et al., 1996).

High permeability of the OMM for K^+ and other small ions may cause a dramatic effect on electrodynamic compartmentation, predicted by computational study of the proposed models (Figs. 4 and 5). Thus, high permeability of the OMM for K^+ leads to a significant redistribution of P_i^-, P_i^{2-}, and PCr^{2-} between the cytoplasm and the MIMS, although it diminishes MDP. This effect of electrodynamic compartmentation of metabolites may be essential for the modulation of corresponding enzymatic reaction rates and hence for cell energy metabolism in general.

In addition, MDP-dependent Ca^{2+} and Mg^{2+} accumulation in the MIMS, according to the Nernst equation, may also play a regulatory role. For example, allosteric Ca^{2+}-dependent enzyme α-glycerophosphate dehydrogenase (Lomax and Robertson, 1990, and references therein), localized on the outer surface of the IMM, may be activated by a MDP-supported higher concentration of Ca^{2+} in the MIMS. Furthermore, Ca^{2+} accumulation in the MIMS may increase the rate of its transport across the IMM and thus may activate some mitochondrial matrix enzymes (Hansford, 1994; McCormack, 1985), thereby increasing the respiration and oxidative phosphorylation rates. Thus, feedback control of the mitochondria metabolic state may be carried out through MDP generation on the OMM.

Furthermore, it is expected that a transitional MDP could be generated during the heart contractile cycle, leading to transitional Ca^{2+} accumulation in the MIMS. Hence, functional interaction between sarcoplasmic reticulum and mitochondria (Landolfi et al., 1998) may work through a transition-state MDP on the OMM. Redistribution of Mg^{2+} ions between the MIMS and the cytoplasm due to steady-state or transition-state MDP may also be essential for the modulation of kinetic parameters of mitochondrial CK and hexokinase (Lipskaya et al., 1995), which could be considered in the future development of the model.

In the case of high OMM permeability for K^+ and other small ions, while the OMMP is diminished, calculations show a pronounced osmotic effect that will increase the MIMS volume (Fig. 5 *E*). Osmotic pressure difference-mediated cyclic flow of solution across the VDAC in the contracting heart could carry out transition-state modulation of the VDAC's permeability by the solute flux (Zizi et al., 1998). Therefore, the MDP-supported osmotic pressure difference on the OMM may be one of the possible explanations of the well-known morphological changes in mitochondria caused by intensive muscle work.

As a result of the MIMS volume increase after a MDP-supported osmotic pressure difference between the MIMS and the cytoplasm, the following regulatory mechanisms, at the level of the OMM, could exist: 1) VDAC voltage sensitivity change due to dilution of the VDAC's modulator(s) and various metabolites in the MIMS; 2) change in the number of intermembrane contact sites; 3) change in the OMM permeability for charged metabolites, via mechanical stress on the OMM caused by the MIMS volume increase; and 4) the matrix volume changes caused by osmotic pressure variations in the MIMS. An increase in the MIMS volume under extreme metabolic conditions may lead to OMM disruption. The probability of OMM damage in a similar process of moderate hypoosmotic swelling of mitochondria was shown to be significantly increased with age and to be higher in male than in female rats (Lemeshko, 1982; Lemeshko and Shekh, 1993).

The simplified cell model (Fig. 2) allows the consideration of the DP and MDP together. The computational study showed that MDP and DP values might be comparable under intensive energy demand in the cytoplasm (Table 2). The DP shifts the PV characteristic of the VDAC to the more sensitive region of VDAC permeability dependence on the OMMP, where the variable MDP component of the OMMP could modulate metabolite flux. In turn, MDP may modulate the DP in some range through MDP-dependent MIMS volume change.

The presented cell model shows the possibility that the energy flux between mitochondria and the cytoplasm may be modulated by the OMM, through the VDAC permeability regulation by generated MDP and an electrodynamic compartmentation effect. Existence of the OMMP seems to be probable, taking into account the presence of the VDAC's voltage-dependent permeability modulators in the MIMS (Liu and Colombini, 1992b; Holden and Colombini, 1993) and the conserved PV characteristics of the VDAC. The considered cell model is very simplified, because it includes only a CK-channeling system, with the concerted functioning of the IMM ATP-synthase and ANT-CK structural complex (Fig. 2 *B*). The main kinetic characteristics of ATP-synthase and ANT-CK structural complex, determined experimentally by other authors (see Aliev and Saks, 1994, and references therein), were used in this model. A more realistic cell model may be developed in the future. It may include the concerted functioning of the IMM ATP-synthase, the ANT-CK complex, and ANT outside of this complex, as well as the fluxes of all adenine nucleotides, PCr, Cr, and P_i through the OMM (Fig. 1 *A*), at different cytosolic workloads. Moreover, the future model may include consideration of equilibrium between cytoplasmic adenine nucleotides and large pools of phosphorylated compounds. The proton-motive force dependence (the IMM potential and ΔpH) on the cytosolic workload may be an additional feedback control on the mitochondrial ATP production. Finally, the matrix volume and the MIMS volume

changes may be modeled as a consequence of electrodynamic compartmentation and osmotic effects. Taking into account all of the above may lead to a more realistic estimation of MDP. Still, the considered simplified cell model shows that the upper value of generated MDP depends mainly on the OMM permeabilities for different charged metabolites and on the cytoplasmic pH at the given workload and energy production rates. The cell model may be developed for transition-state MDP generation as well, describing MDP oscillations in accordance with heart contractions.

APPENDIX A: EQUATIONS FOR THE ESTIMATED RATES OF ATP AND PCr PRODUCTION BY RAT HEART AVERAGE MITOCHONDRION

Free energy of ATP hydrolysis in rat heart ventricular sarcoplasm for the resting state was determined to be −61.9 kJ/mol by extrapolation from experimental data (Tian and Ingwall, 1996). Therefore, if

$$\Delta G' = \Delta G^{\circ\prime} + RT \cdot \ln \frac{[\mathrm{ADP}]_o \cdot [\mathrm{P_i}]_o}{[\mathrm{ATP}]_o}, \tag{A1}$$

where $\Delta G^{\circ\prime} = -30.5$ kJ/mol, then

$$\log \frac{[\mathrm{ADP}]_o \cdot [\mathrm{P_i}]_o}{[\mathrm{ATP}]_o} = \frac{-61.9 + 30.5}{2.3 \cdot 0.0083 \cdot 310} = -5.3, \tag{A2}$$

or in another form,

$$\frac{[\mathrm{ADP}]_o \cdot [\mathrm{P_i}]_o}{[\mathrm{ATP}]_o} = 10^{-5.3} = 5 \times 10^{-6}. \tag{A3}$$

Rat heart mitoplasts are able to maintain the mass action ratio of CK reaction coupled with the oxidative phosphorylation system at the level of 0.017 (Saks and Aliev, 1996). Extrapolating the data (Saks and Aliev, 1996) to a zero rate of the total PCr production, we obtained the following relationship for a near-equilibrium state of this system:

$$\frac{[\mathrm{PCr}][\mathrm{ADP}]}{[\mathrm{Cr}][\mathrm{ATP}]} = 0.019. \tag{A4}$$

Combining two reactions, the reaction

$$\mathrm{P_i} + \mathrm{ADP} = \mathrm{ATP} + \mathrm{H_2O} \tag{A5}$$

with $K_{eq,1} = 2 \times 10^5\ \mathrm{M}^{-1}$, according to Eq. A3, and the reaction

$$\mathrm{Cr} + \mathrm{ATP} = \mathrm{PCr} + \mathrm{ADP} \tag{A6}$$

with $K_{eq,2} = 1.9 \times 10^{-2}$, according to Eq. A4, into one reaction yields

$$\mathrm{Pi} + \mathrm{Cr} = \mathrm{PCr} + \mathrm{H_2O}, \tag{A7}$$

with $K_{eq} = (2 \times 10^5) \times (1.9 \times 10^{-2}) = 3.8 \times 10^3\ \mathrm{M}^{-1}$.

By taking the sarcoplasmic concentrations of $[\mathrm{PCr}]_o = 0.019$ M and $[\mathrm{Cr}]_o = 0.009$ M, which are known to be maintained in rat heart at rest, it is possible to calculate the sarcoplasmic concentration of $[\mathrm{P_i}]_o$ in the resting state according to Eq. A7 (approximation of resting state to equilibrium is done by taking $v_{max,o} = 0$):

$$[\mathrm{P_i}]_o = \frac{0.019\ \mathrm{M}}{0.009\ \mathrm{M} \times 3.8 \times 10^3\ \mathrm{M}^{-1}} = 0.00056\ \mathrm{M}. \tag{A8}$$

The steady-state rate of ATP production, v_{ATP}, by mitochondria may be approximated by the following formula, as an essentially reversible reaction:

$$v_{ATP} = \frac{\dfrac{[\mathrm{P_i}]_m \cdot [\mathrm{ADP}]_m \cdot v_{max,m,f}}{K_{m,P_i} \cdot K_{m,ADP}} - \dfrac{[\mathrm{ATP}]_m \cdot v_{max,m,r}}{K_{m,ATP}}}{1 + \dfrac{[\mathrm{ATP}]_m}{K_{m,ATP}} + \dfrac{[\mathrm{ADP}]_m}{K_{m,ADP}} + \dfrac{[\mathrm{ADP}]_m \cdot [\mathrm{P_i}]_m}{K_{m,ADP} \cdot K_{m,P_i}}}. \tag{A9}$$

Here, $v_{max,m,f}$ is the maximum rate of the forward reaction, i.e., the reaction of ATP production from ADP and P_i; $v_{max,m,r}$ is the maximum rate of the reverse reaction; $[ATP]_m$, $[ADP]_m$, and $[P_i]_m$ are ATP, ADP, and P_i concentrations in the mitochondrial matrix, and $K_{m,ATP}$, $K_{m,ADP}$, and $K_{m,Pi}$ are K_m values for ATP, ADP, and P_i, respectively. For the rat heart mitochondrial matrix, K_m values have been reported to have the following values (see Saks and Aliev, 1996): $K_{m,ATP} = 0.000462$ M; $K_{m,ADP} = 0.0001$ M; $K_{m,Pi} = 0.0024$ M.

ADP concentration near myofibrils in rat heart may be estimated as $[ADP]_o = 0.00004$ M, which is close to the experimental data (Saks and Aliev, 1996). In the limit situation, when there is no utilization of PCr in the cytoplasm, ADP concentration in the MIMS was accepted to be the same as in the cytoplasm: $[ADP]_i = [ADP]_o = 0.00004$ M.

In accordance with Saks and Aliev (1996), ADP concentration in the mitochondrial matrix, $[ADP]_m$, is ~25 times higher than in the MIMS; therefore $[ADP]_m = 0.00004 \times 25 = 0.001$ M. ATP concentration in the rat heart sarcoplasm is usually found to be near 0.01 M. The sum of the matrix ATP and matrix ADP concentrations is taken to be constant and equal to 0.01 M, i.e., $[ATP]_m + [ADP]_m = 0.01$ M (Saks and Aliev, 1996). Because $[ADP]_m$ has been already calculated to be 0.001 M, $[ATP]_m$ should be 0.009 M to satisfy the last equation. The P_i concentration in the matrix is ~10 times higher than in the MIMS, i.e., $[P_i]_m = 10[P_i]_i$ (Saks and Aliev, 1996).

Thus, assuming $v_{max,m,f} = v_{max,m,r} = v_{max,m}$, Eq. (A9) can be rewritten in the following form:

$$\begin{aligned} v_{ATP} &= \frac{\dfrac{10 \cdot [\mathrm{P_i}]_i \cdot 25 \cdot [\mathrm{ADP}]_i \cdot v_{max,m,f}}{K_{m,P_i} \cdot K_{m,ADP}} - \dfrac{[\mathrm{ATP}]_m \cdot v_{max,m,r}}{K_{m,ATP}}}{1 + \dfrac{[\mathrm{ATP}]_m}{K_{m,ATP}} + \dfrac{25 \cdot [\mathrm{ADP}]_i}{K_{i,ADP}} + \dfrac{25 \cdot [\mathrm{ADP}]_i \cdot 10 \cdot [\mathrm{P_i}]_i}{K_{m,ADP} \cdot K_{m,P_i}}} \\ &= \frac{v_{max,m} \cdot (41{,}667 \cdot [\mathrm{P_i}]_i - 19.5)}{41{,}667 \cdot [\mathrm{P_i}]_i + 30.5}. \end{aligned} \tag{A10}$$

Equation A10 shows how P_i regulates ATP production by mitochondria in a crude approximation. If net ATP production becomes 0, then regardless of $v_{max,m}$, Eq. A10 yields $[P_i]_i = 0.00047$ M in the MIMS, which is close to $[P_i]_i = 0.00056$ M, obtained from Eq. A8. Thus, the approximations and equations above are adequate and consistent with each other.

According to Aliev and Saks (1994), the rate of the MIMS-CK reaction

$$\mathrm{ATP_i} + \mathrm{Cr_i} = \mathrm{ADP_i} + \mathrm{PCr_i}$$

is described by the following equation:

$$v_i = \frac{\dfrac{[\mathrm{ATP}]_i \cdot [\mathrm{Cr}]_i \cdot v_{max,i,f}}{K_{ia} \cdot K_{cr}} - \dfrac{[\mathrm{PCr}]_i \cdot [\mathrm{ADP}]_i \cdot v_{max,i,r}}{K_{cp} \cdot K_{id}}}{Den}. \tag{A11}$$

Assuming that the forward rate of the MIMS-CK reaction is limited by the rate of ATP production by mitochondria, the maximum rate $v_{max,i,f}$ of the MIMS-CK reaction in Eq. A11 can be replaced by Eq. A10:

$$v_i = \frac{v_{max,m} \cdot (41{,}667 \cdot [P_i]_i - 19.5) \cdot [ATP]_i \cdot [Cr]_i}{(41{,}667 \cdot [P_i]_i + 30.5) \cdot K_{ia} \cdot K_{cr}} - \frac{[PCr]_i \cdot [ADP]_i \cdot v_{max,i,r}}{K_{cp} \cdot K_{id}}, \quad (A12)$$

where

$$Den = 1 + \frac{[Cr]_i}{K_{icr}} + \frac{[ATP]_i}{K_{ia}} + \frac{[ATP]_i \cdot [Cr]_i}{K_{ia} \cdot K_{cr}} + \frac{[PCr]_i}{K_{icp}} + \frac{[PCr]_i \cdot [ATP]_i}{K_{icp} \cdot K_{Ia}} + \frac{[ADP]_i}{K_{id}} + \frac{[ADP]_i \cdot [PCr]_i}{K_{id} \cdot K_{cp}} + \frac{[ADP]_i \cdot [Cr]_i}{K_{id} \cdot K_{Icr}}. \quad (A13)$$

Now, one can include in Eqs. A12 and A13 the values of metabolite concentrations mentioned above and the kinetic constants, equal or close to those reported elsewhere for the mitochondrial CK reaction coupled with the oxidative phosphorylation system through ANT (Aliev and Saks, 1994; Saks and Aliev, 1996): $v_{max,m} = 0.0067$ fmol/s (calculated for one average mitochondrion; see Appendix B); $v_{max,i,r} = 0.0133$ fmol/s (calculated for one average mitochondrion; see Appendix B); $[ATP]_i = 0.01$ M, $[ADP]_i = 0.00004$ M; $K_{icr} = 0.030$ M; $K_{ia} = 0.00015$ M; $K_{cr} = 0.0052$ M; $K_{icp} = 0.0014$ M; $K_{cp} = 0.001$ M; $K_{Ia} = 0.01125$ M; $K_{id} = 0.000208$ M; $K_{Icr} = 0.0052$ M.

After we make the substitutions above, Eq. A13 becomes

$$Den = 67.7 + 12{,}890 \cdot [Cr]_i + 1541 \cdot [PCr]_i. \quad (A14)$$

Taking $[Cr]_i = 0.009$ M and $[PCr]_i = 0.019$ M for the resting state modeled by making $v_i = 0$, Eq. A12 is satisfied when $[P_i]_i = 0.00055$ M, which is approximately the same value as $[P_i]_i = 0.00056$ M, calculated above for the case where $v_{max,o} = 0$ in Eq. A8. Thus, the two conditions, $v_i = 0$ and $v_{max,o} = 0$, gave the same result for $[P_i]_i$. It is taken into account that

$$[P_i] = [P_i^-] + [P_i^{2-}]. \quad (A15)$$

Knowing $pK_{a2} = 7.21$ for P_i, $[P_i^-]$ can be expressed through $[P_i]_i$ and H^+ concentration in the medium:

$$[P_i^-] = \frac{[P_i]}{1 + [H^+]/0.62 \times 10^{-7}}. \quad (A16)$$

The cytoplasm pH was assumed to be constant and equal to 7.0 in most calculations, except where it was varied in the range of 6.5–7.5 (Table 2). The MIMS pH value, pH_i, will depend on the relationship of $[P_i^-]_i$ and $[P_i^{2-}]_i$ in the MIMS.

APPENDIX B: ESTIMATION OF MITOCHONDRIAL VOLUME, MAXIMUM RATES OF FORWARD AND REVERSE MIMS-CK REACTION, AND THE OMM PERMEABILITY

The average effective diameter of rat heart mitochondrion is 0.61 μm (Smith and Page, 1976). Therefore, the average volume of one mitochondrion, V_{mit}, is equal to

$$V_{mit} = \frac{\pi \cdot d^3}{6} = \frac{\pi \cdot (0.61\ \mu m)^3}{6} = 0.12\ \mu m^3 = 0.12\ fl. \quad (B1)$$

The mitochondrial matrix volume is ~1.5–2 μl/mg of mitochondrial protein (Crompton et al., 1987a, 1987b). It was assumed that the matrix volume was three-fourths of the mitochondrion volume and that a mitochondrion volume of 2 μl contained 1 mg of mitochondrial protein. The average protein mass of a single mitochondrion in rat heart, m_{mit}, can now be calculated, taking into account Eq. B1:

$$m_{mit} = \frac{1\ mg}{2\ \mu l} \times 0.12\ fl = 60 \times 10^{-12}\ mg. \quad (B2)$$

It is known that 60 mg of mitochondrial protein corresponds to 1 g wm of rat heart tissue (Saks and Aliev, 1996). Therefore, the mass of rat heart tissue corresponding on the average to one mitochondrion, $m_{rh/m}$, can be calculated:

$$m_{rh/m} = 1\ g\ wm \cdot \frac{60 \times 10^{-12}\ mg}{60\ mg} = 10^{-12}\ g\ wm. \quad (B3)$$

Thus, there is one mitochondrion per 10^{-12} g wm of rat heart tissue.

The maximum rate of ATP production by the MIMS CK is 13.3 μmol s^{-1} (g wm)$^{-1}$ (Saks and Aliev, 1996), from which, together with Eq. B3, the MIMS-CK maximum rate of ATP production by a single mitochondrion, $v_{max,i,r}$ (see Eq. A11), is calculated:

$$v_{max,i,r} = 13.3 \frac{\mu mol\ ATP \cdot m_{rh/m}}{s \cdot g\ wm} = 13.3 \times 10^{-12} \frac{\mu mol\ ATP}{s}\ \text{per mitochondrion} = 0.0133\ \frac{fmol}{s}\ \text{per mitochondrion}. \quad (B4)$$

Because the maximum rate of the MIMS-CK forward reaction, i.e., PCr production, is limited mostly by the rate of oxidative phosphorylation or by ANT, $v_{max,i,f} = v_{ATP}$ (see Eqs. A10 and A11). The rate v_{ATP} is limited by the maximum rate of ATP production in mitochondria, $v_{max,m}$. The rate $v_{max,m}$ was set at $v_{max,m} = v_{max,i,r}/2 = 0.0067$ fmol/s per mitochondrion, because it is close to the experimentally measured value and because, when it is used in Eq. A11, v_i becomes 0 when $[P_i]_i = 0.00055$ M, which is very close to $[P_i]_i = 0.00056$ M for $v_{max,o} = 0$, calculated independently for Eq. A8.

The molecular mass of the VDAC is ~30,000 Da (Colombini et al., 1996), which corresponds to the mass of a single VDAC channel of 30×10^3 Da/$(6.022 \times 10^{23}) = 5 \times 10^{-17}$ mg. It is known that the VDAC constitutes ~0.3% of mitochondrial proteins by mass (Linden et al., 1984); therefore the number of VDAC channels per mitochondrion, n, can be estimated by using the result from Eq. (B2):

$$n = \frac{0.003 \times 60 \times 10^{-12}\ mg}{5 \times 10^{-17}\ mg} = 3600. \quad (B5)$$

Reconstituted in a planar lipid bilayer, the VDAC has permeability for P_i^{2-} in the open state at zero membrane potential $P_{P_i}^{2-} = 10^{-14}$ cm^3/s (Rostovtseva and Colombini, 1997). Therefore, if it is assumed that the VDAC is the major channel for metabolite flow through the OMM, and that it behaves the same way in vivo as in the planar lipid bilayer, then the maximum absolute permeability of a single mitochondrion's OMM for P_i^{2-}

should be $P^{2-}_{P_i}$ max $= 3600 \times 10^{-14}$ cm^3/s $= 36$ fl/s. In the simplified cell model, $P^{2-}_{P_i}$ was taken to be one order of magnitude lower than the maximum calculated OMM permeability corresponding to a completely open state of the VDAC. There are data indicating that the VDAC in vivo may behave very differently from how it behaves in vitro. Specifically, the VDAC has been shown to regulate the activity of mitochondrial respiration by reducing the outer membrane permeability (Liu and Colombini, 1991, 1992a, 1992b). Studies of reconstituted VDAC revealed that the channel might stay in the completely closed state longer than was previously thought (Bathori et al., 1998). It is not excluded that even in the closed state VDAC permeability may be further diminished by some of the regulatory factors in the MIMS and/or in the cytoplasm.

We thank Dr. Marco Colombini for his support at the beginning of this project, for helpful discussions, critical reading of the manuscript, and for providing the data about VDAC permeability in the open and closed states for phosphocreatine.

SVL is a Baylor Research Advocates for Student Scientists scholar at the Graduate School of Biomedical Sciences at Baylor College of Medicine, Houston, TX. VVL was supported by Colciencias grant 1118-05-261-97.

REFERENCES

Aliev, M. K., and V. A. Saks. 1994. Mathematical modeling of intracellular transport processes and the creatine kinase systems: a probability approach. *Mol. Cel. Biochem.* 133/134:333–346.

Bathori, G., I. Szabo, I. Schmehl, F. Tombola, A. Messina, V. De Pinto, and M. Zoratti. 1998. Novel aspects of the electrophysiology of mitochondrial porin. *Biochem. Biophys. Res. Commun.* 243:258–263.

Benz, R., M. Kottke, and D. Brdiczka. 1990. The cationically selective state of the mitochondrial outer membrane pore: a study with intact mitochondria and reconstituted mitochondrial porin. *Biochim. Biophys. Acta.* 1022:311–318.

Brdiczka, D., and T. Wallimann. 1994. The importance of the outer mitochondrial compartment in regulation of energy metabolism. *Mol. Cell. Biochem.* 133/134:69–83.

Colombini, M. 1979. A candidate for the permeability pathway of the outer mitochondrial membrane. *Nature.* 279:643–645.

Colombini, M., E. Blachly-Dyson, and M. Forte. 1996. VDAC, a channel in the outer mitochondrial membrane. *In* Ion Channels, Vol. 4. T. Narahashi, editor. Plenum Press, New York. 169–202.

Colombini, M., C. L. Yeung, J. Tung, and T. Konig. 1987. The mitochondrial outer membrane channel, VDAC, is regulated by a synthetic polyanion. *Biochim. Biophys. Acta.* 905:279–286.

Crompton, M., A. Costi, and L. Hayat. 1987a. Evidence for presence of reversible Ca^{2+}-dependent pore activated by oxidative stress in heart mitochondria. *Biochem. J.* 245:915–918.

Crompton, M., A. Costi, and L. Hayat. 1987b. A reversible Ca^{2+}-dependent pore activated by oxidative stress in heart mitochondria. *Biochem. Soc. Trans.* 15:408–409.

Hansford, R. G. 1994. Physiological role of mitochondrial Ca^{2+} transport. *J. Bioenerg. Biomembr.* 26:495–508.

Hodge, T., and M. Colombini. 1997. Regulation of metabolite flux through voltage-gating of VDAC channels. *J. Membr. Biol.* 157:271–279.

Holden, M. J., and M. Colombini. 1993. The outer mitochondrial channel, VDAC, is modulated by a protein localized in the intermembrane space. *Biochim. Biophys. Acta.* 1144:396–402.

Landolfi, B., S. Curci, L. Debellis, T. Pozzan, and A. M. Hofer. 1998. Ca^{2+} homeostasis in the agonist-sensitive internal store: functional interactions between mitochondria and the ER measured in situ in intact cells. *J. Cell. Biol.* 142:1235–1243.

Lee, A. C., X. Xu, and M. Colombini. 1996. The role of pyridine dinucleotides in regulating the permeability of the mitochondrial outer membrane. *J. Biol. Chem.* 271:26724–26731.

Lemeshko, V. V. 1982. Dependence of the structural lability of the outer membrane of liver mitochondria on the age and sex of rats. *Biofizika.* 27:837–840.

Lemeshko, V. V., and V. E. Shekh. 1993. Hypotonic fragility of outer membrane and activation of external pathway of NADH oxidation in rat liver mitochondria are increased with age. *Mech. Ageing Dev.* 68: 221–233.

Linden, M., G. Andersson, P. Gellerfors, and B. D. Nelson. 1984. Subcellular distribution of rat liver porin. *Biochim. Biophys. Acta.* 770:93–96.

Lipskaya, T. Yu., P. J. Geiger, and S. P. Bessman. 1995. Compartmentation and metabolic parameters of mitochondrial hexokinase and creatine kinase depend on the rate of oxidative phosphorylation. *Biochem. Mol. Med.* 55:81–89.

Liu, M. Y., and M. Colombini. 1991. Voltage gating of the mitochondrial outer membrane channel VDAC is regulated by a very conserved protein. *Am. J. Physiol.* 260(2 Pt 1):C371–C374.

Liu, M. Y., and M. Colombini. 1992a. Regulation of mitochondrial respiration by controlling the permeability of the outer membrane through the mitochondrial channel, VDAC. *Biochim. Biophys. Acta.* 1098:255–260.

Liu, M. Y., and M. Colombini. 1992b. A soluble mitochondrial protein increases the voltage dependence of the mitochondrial channel. VDAC. *J. Bioenerg. Biomembr.* 24:41–46.

Lomax, R. B., and W. R. Robertson. 1990. Mitochondrial α-glycerol phosphate dehydrogenate activity in IIA fibers of the rat lateral gastrocnemius muscle; the effect of Ca^{2+} and ATP. *Histochem. J.* 22:119–124.

Mangan, P. S., and M. Colombini. 1987. Ultrasteep voltage dependence in a membrane channel. *Proc. Natl. Acad. Sci. USA.* 84:4896–4900.

Mannella, C. A. 1982. Structure of the outer mitochondrial membrane: ordered arrays of porelike subunits in outer-membrane fractions from *Neurospora crassa* mitochondria. *J. Cell Biol.* 94:680–687.

Mannella, C. A., M. Forte, and M. Colombini. 1992. Toward the molecular structure of the mitochondrial channel, VDAC. *J. Bioenerg. Biomembr.* 24:7–19.

McCormack, J. G. 1985. Evidence that adrenaline activates key oxidative enzymes in rat liver by increasing intramitochondrial [Ca^{2+}]. *FEBS Lett.* 180:259–264.

O'Gorman, E., G. Beutner, T. Wallimann, and D. Brdiczka. 1996. Differential effects of creatine depletion on the regulation of enzyme activities and on creatine-stimulated mitochondrial respiration in skeletal muscle, heart, and brain. *Biochim. Biophys. Acta.* 1276:161–170.

Rostovtseva, T. K., and S. M. Bezrukov. 1998. ATP transport through a single mitochondrial channel, VDAC, studied by current fluctuation analysis. *Biophys. J.* 74:2365–2373.

Rostovtseva, T., and M. Colombini. 1997. VDAC channels mediate and gate the flow of ATP: implications for the regulation of mitochondrial function. *Biophys. J.* 72:1954–1962.

Saks, V. A. and M. K. Aliev. 1996. Is there the creatine kinase equilibrium in working heart cells? *Biochem. Biophys. Res. Commun.* 227(2): 360–367.

Saks, V. A., Z. A. Khuchua, E. V. Vasilyeva, O. Yu. Belikova, and A. V. Kuznetsov. 1994. Metabolic compartmentation and substrate channelling in muscle cells. Role of coupled creatine kinases in in vivo regulation of cellular respiration—a synthesis. *Mol. Cell. Biochem.* 133–134: 155–192.

Saks, V. A., A. V. Kuznetsov, Z. A. Khuchua, E. V. Vasilyeva, J. O. Belikova, T. Kesvatera, and T. Tiivel. 1995. Control of cellular respiration in vivo by mitochondrial outer membrane and by creatine kinase. A new speculative hypothesis: possible involvement of mitochondrial-cytoskeleton interactions. *J. Mol. Cell. Cardiol.* 27:625–645.

Saks, V. A., A. V. Kuznetsov, V. V. Kupriyanov, M. V. Miceli, and W. E. Jacobus. 1985. Creatine kinase of rat heart mitochondria. The demonstration of functional coupling to oxidative phosphorylation in an inner membrane-matrix preparation. *J. Biol. Chem.* 260:7757–7764.

Saks, V. A., E. Vasil'eva, Yu. O. Belikova, A. V. Kuznetsov, S. Lyapina, L. Petrova, and N. A. Perov. 1993. Retarded diffusion of ADP in cardiomyocytes: possible role of mitochondrial outer membrane and creatine kinase in cellular regulation of oxidative phosphorylation. *Biochim. Biophys. Acta.* 1144:134–148.

Schein, S. J., M. Colombini, and A. Finkelstein. 1976. Reconstitution in planar lipid bilayers of a voltage-dependent anion-selective channel, obtained from Paramecium mitochondria. *J. Membr. Biol.* 30:99–120.

Smith, H. E., and E. Page. 1976. Morphometry of rat heart mitochondrial subcompartments and membranes: application to myocardial cell atrophy after hypophysectomy. *J. Ultrastruct. Res.* 55:31–41.

Sorgato, M. C., and O. Moran. 1993. Channels in mitochondrial membranes: knowns, unknowns, and prospects for the future. *Crit. Rev. Biochem. Mol. Biol.* 28:127–171.

Tian, R., and J. S. Ingwall. 1996. Energetic basis for reduced contractile reserve in isolated rat hearts. *Am. J. Physiol.* 270(4 Pt 2):H1207–H1216.

Wallimann, T., M. Wyss, D. Brdiczka, K. Nikolay, and H. M. Eppenberger. 1992. Intracellular compartmentation, structure and function of creatine kinase isoenzymes in tissues with high and fluctuating energy demands: the "phosphocreatine circuit" for cellular energy homeostasis. *Biochem. J.* 281(Pt 1):21–40.

Zimmerberg, J., and V. A. Parsegian. 1986. Polymer inaccessible volume changes during opening and closing of a voltage-dependent ionic channel. *Nature.* 323:36–39.

Zizi, M., C. Byrd, R. Boxus, and M. Colombini. 1998. The voltage-gating process in the voltage-dependent anion channel is sensitive to ion flow. *Biophys. J.* 75:704–713.

Zizi, M., L. Thomas, E. Blachly-Dyson, M. Forte, and M. Colombini. 1995. Oriented channel insertion reveals the motion of a transmembrane beta strand during voltage gating of VDAC. *J. Membr. Biol.* 144: 121–129.